AD-A200 753

RADC-TR-88-92
Final Technical Report
June 1988

IMPEDANCE MATCHING FOR HIGH SPEED OPTICAL COMMUNICATION

Stevens Institute of Technology

Dr. Henry Zmuda

APPROVED FOR PUBLIC RELEASE; DISTRIBUTION UNLIMITED.

ROME AIR DEVELOPMENT CENTER
Air Force Systems Command
Griffiss Air Force Base, NY 13441-5700

DTIC
ELECTE
OCT 1 8 1988
H

88 10 18 105

REPORT DOCUMENTATION PAGE

Form Approved
OMB No. 0704-0188

1a. REPORT SECURITY CLASSIFICATION	1b. RESTRICTIVE MARKINGS
UNCLASSIFIED	N/A

2a. SECURITY CLASSIFICATION AUTHORITY	3. DISTRIBUTION/AVAILABILITY OF REPORT
N/A	Approved for public release;
2b. DECLASSIFICATION/DOWNGRADING SCHEDULE	distribution unlimited.
N/A	

4. PERFORMING ORGANIZATION REPORT NUMBER(S)	5. MONITORING ORGANIZATION REPORT NUMBER(S)
N/A	RADC-TR-88-92

6a. NAME OF PERFORMING ORGANIZATION	6b. OFFICE SYMBOL (If applicable)	7a. NAME OF MONITORING ORGANIZATION
Stevens Institute of Technology		Rome Air Development Center (DCLW)

6c. ADDRESS (City, State, and ZIP Code)	7b. ADDRESS (City, State, and ZIP Code)
Department of Electrical Engineering and Computer Science Hoboken NJ 07030	Griffiss AFB NY 13441-5700

8a. NAME OF FUNDING/SPONSORING ORGANIZATION	8b. OFFICE SYMBOL (If applicable)	9. PROCUREMENT INSTRUMENT IDENTIFICATION NUMBER
Rome Air Development Center	DCLW	F30602-81-C-0185

8c. ADDRESS (City, State, and ZIP Code)	10. SOURCE OF FUNDING NUMBERS			
Griffiss AFB NY 13441-5700	PROGRAM ELEMENT NO	PROJECT NO.	TASK NO	WORK UNIT ACCESSION NO.
	63726F	2863	92	P3

11. TITLE (Include Security Classification)

IMPEDANCE MATCHING FOR HIGH SPEED OPTICAL COMMUNICATION

12. PERSONAL AUTHOR(S)
Dr. Henry Zmuda

13a. TYPE OF REPORT	13b. TIME COVERED	14. DATE OF REPORT (Year, Month, Day)	15. PAGE COUNT
Final	FROM Apr 87 TO Oct 87	June 1988	50

16. SUPPLEMENTARY NOTATION
This effort was performed as a Post-Doctoral study by Stevens Institute of Technology under a Georgia Institute of Technology contract.

17.	COSATI CODES		18. SUBJECT TERMS (Continue on reverse if necessary and identify by block number)
FIELD	GROUP	SUB-GROUP	Non-Radio Communications Lasers
25	03		Optical Communications Integrated Optics
20	06	01	Fiber Optics

19. ABSTRACT (Continue on reverse if necessary and identify by block number)

This technical report details several methods of providing low Standing Wave Ratio (SWR), low loss, broadband microwave impedance matching for direct modulation of a laser diode. The report addresses group delay performance of matching networks and provides several Computer-Aided-Designs (CAD) solutions to impedance matching of the laser diodes in both active and passive systems.

20. DISTRIBUTION/AVAILABILITY OF ABSTRACT	21. ABSTRACT SECURITY CLASSIFICATION
☐ UNCLASSIFIED/UNLIMITED ☒ SAME AS RPT ☐ DTIC USERS	UNCLASSIFIED

22a. NAME OF RESPONSIBLE INDIVIDUAL	22b. TELEPHONE (Include Area Code)	22c. OFFICE SYMBOL
Norman P. Bernstein	(315) 330-4092	RADC (DCLW)

DD Form 1473, JUN 86   Previous editions are obsolete.   SECURITY CLASSIFICATION OF THIS PAGE

UNCLASSIFIED

TABLE OF CONTENTS

List of Illustrations

Elements specified in terms of normalized values: R/R_o, $\omega_o CR_o$ and $\omega_o L/R_o$, R_o, ω_o arbitrary real positive constants

I. INTRODUCTION

The problem of broad-band matching a frequency dependent generator and load has been the subject of extensive study. [1-5] The situation to be studied can be concisely understood by examination of figure 1a, where z_1 represents a specified load impedance and z_g and e_g can be thought of as the Thevenin equivalent circuit of a source network. It is assumed that both that both z_g and z_1 are passive (non-Foster) impedances, though this assumption will be relaxed later. Darlington's theorem states that any passive impedance function can always be realized as the input impedance of a lossless two-port terminated in a pure resistance. Figure 1b thus shows a Darlington representation of the generator and load impedances. The classical broad-band matching problem has been to determine a lossless two-port matching network E so as to achieve maximum power transfer between e_g and R_1 over a prescribed frequency band.[1]

Since most modern communications systems involve the high speed transmission of digital data, pulse properties such as rise time, pulse width, settling time, etc. are often the primary design requirements. Although the time and frequency domains are linked through a Fourier transform, the classical broad-band matching techniques do not allow immediate control of the time domain.

A separate though related question is concerned with the phase or delay characteristics of a transmission system.[2]

---

[1]Maximum power transfer here is defined as the ratio of average power delivered to R_1 to the maximum available power from e_g.

[2]For $H(\omega) = |H(\omega)|\exp(j\psi(\omega))$, the phase response is $\psi(\omega)$ and the group delay is $\tau(\omega) = d\psi(\omega)/d\omega$.
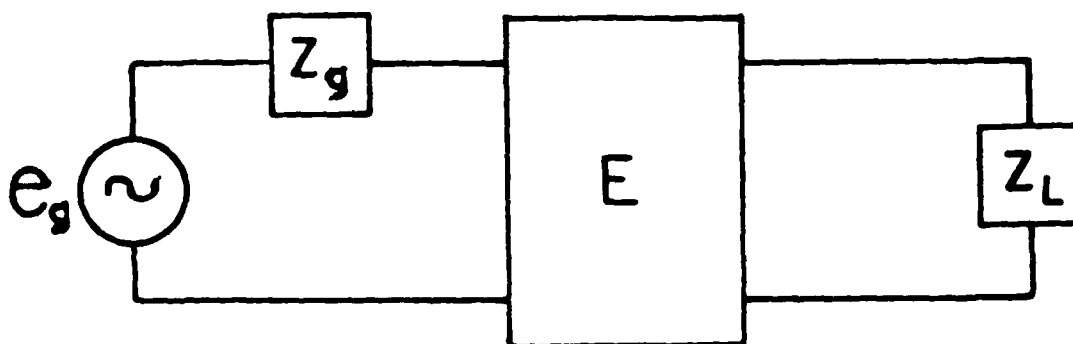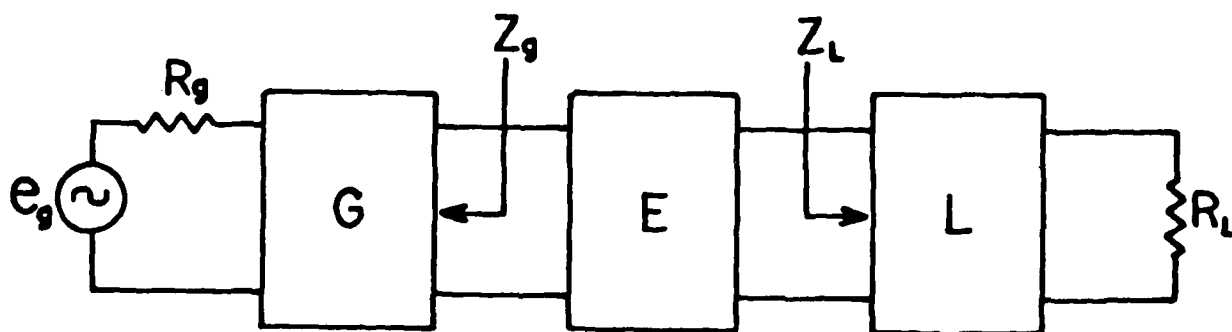
Figure 1-a: The General Matching Problem

Figure 1-b: Darlington representation of generator and load impedances

Clearly, for phase modulated systems, the group delay characteristics take priority over the amplitude performance. To date, relatively little is known on the design of matching networks operating between frequency dependent terminations which yield specified group delay performance. [6]

This report addresses each of the above concerns, and presents numerical (CAD) procedures for the design of broad-band matching networks with either the system's time domain performance (impulse response synthesis) or group delay as the primary concern. Since many of the commonly sought frequency domain properties have an equivalent time domain interpetation, the procedures developed offer a fresh perspective to classical broadband matching problems.

Since the final network synthesis process must of course be carried out in the frequency domain, maximum advantage is taken of the wealth of CAD procedures extant. [7]

Finally, several examples are included which illustrate the techniques developed specifically for the case of high speed fiber optic communication links, including the design of active equalization.

II. Equalizer Properties

The design of networks which approximate a specified frequency response, phase response or impulse response all involve the determination of the matching network E of figure 1. This section examines the properties E must have to ensure that the resulting design will be realizable. To this end consider the real normalized scattering matrix of a two-port network.

$$S = (s_{ij}) \; ; \; i,j = 1,2 \tag{1}$$

From this S matrix one can readily compute the corresponding transfer scattering matrix [8]

$$T = (t_{i,j}) \; ; \; i,j = 1,2 \tag{2a}$$

where

$$t_{11} = \Delta s/s_{21} \; , \; t_{12} = s_{11}/s_{21} \tag{2b}$$

$$t_{21} = -s_{22}/s_{21} \; , \; t_{22} = 1/s_{21}$$

$$\Delta s = s_{12} \, s_{21} - s_{11} \, s_{22}$$

and

$$s_{11} = t_{12}/t_{22} \; , \; s_{12} = \Delta t/s_{22} \tag{2c}$$

$$s_{21} = 1/t_{22} \; , \; s_{22} = - \, t_{21}/t_{22}$$

$$\Delta t = t_{12} \, t_{21} - t_{11} \, t_{22}$$

These transmission parameters are useful for determining the overall scattering matrix of a cascade of two-port networks in that the transfer scattering matrix for the overall system is simply the product of the individual transfer scattering matrices. It is tactily assumed that common ports share the same normalization.

Consider then the G-E-L cascade of figure 1b. Assume that generator, equalizer and load have scattering matrices,

respectively as

$$S_g = (g_{ij})$$

$$S_e = (e_{ij}) \; ; \; i,j = 1,2 \tag{3}$$

$$S_l = (l_{ij})$$

It is assumed that S_g and S_l are known, S_e is unknown. The transfer scattering matrix for the overall G-E-L cascade is simply

$$T = T_g T_e T_l \tag{4}$$

where T_g, T_e and T_l are computed via eq. (2b) and the overall scattering matrix is then computed from eq. (2c). Only the (2,1) element (the transmittance) is of interest here and is computed as

$$s_{21}(s) = \frac{g_{21} e_{21} l_{21}}{1 - g_{22} l_{11} \Delta e - g_{22} e_{11} - e_{22} l_{11}} \tag{5}$$

where $\Delta e = e_{21}^2 - e_{22} e_{11}$

Though $S_e = (e_{ij})$ is unknown, it represents the scattering matrix of a lossless reciprocal two-port network. This requires that $S_e(s)$ be unitary,

$$I - S_e^+(s) S_e(s) \tag{6}$$

where $()^+$ means conjugate transpose and I is the 2x2 identity matrix. Imposing the condition the S_e be rational, (6) yields the canonic representation

$$S_e = \frac{1}{g(s)} \begin{bmatrix} h(s) & f(s) \\ \pm f(-s) & h(-s)f(s)/f(-s) \end{bmatrix} \qquad (7)$$

where

> f,g and h are polynomials g(s) is strictly Hurwitz and
> of degree n, $s = \sigma + j\omega$

and (6) requires that f, g and h satisfy

$$h(s)h(-s) \pm f^2(s) = g(s)g(-s). \qquad (8)$$

The polynomial f(s) is further restricted in that any zeros of f(s) in Re(s) < 0 must appear in image pairs. This will not be of concern here since it is assumed that E is a minimum phase structure with all zeros of transmission of $e_{21}(s)$ at zero or infinity. This gives

$$f(s) = s^k , \quad 0 \leq k \leq n \qquad (9)$$

This restriction will yield E as a ladder structure easily implemented with transmission lines of commensurate length. A more general form for f(s) would most likely require coupled coils in a realization, and is not feasible at microwave frequencies.

Hence the form of the scattering matrix of E is

$$S_e = \frac{1}{g(s)} \begin{bmatrix} h(s) & s^k \\ s^k & -(-1)^k h(-s) \end{bmatrix} \qquad (10a)$$

with
$$g(s)g(-s) = h(s)h(-s) + s^{2k} \qquad (10b)$$

Any S_e satisfying (10) will guarantee realizability.

It should be noted that n, the degree of g(s) is the number of elements (capacitors and inductors) in E and k is the number of high pass (series capacitors, shunt inductors) in E. Thus k = 0 is low pass, 0 < k < n is band pass, and k = n is high pass, all in the form of a ladder topology.

Note also that once h(s) and g(s) are determined, the synthesis is immediate, since

$$z_{in} = [1 + e_{11}(s)]/[1 - e_{11}(s)]$$

$$= [g(s) + h(s)]/[g(s) - h(s)] \qquad (11)$$

which can always be realized as the input impedance of a lossless two-port terminated in a resistor by Darlington synthesis. The lossless network with the resistor removed is the matching network E.

III Impulse Response Synthesis

Consider the problem of specifying an impulse response $h(t)$.[9] In the development which follows, $h(t)$ will be related to the power delivered to a resistive load when the input power is impulsive in nature. Specifically, incident wave variables $a_1(t)$, $a_2(t)$ and reflected wave variables $b_1(t)$, $b_2(t)$ are related through the scattering matrix in the usual way as

$$
\begin{bmatrix} b_1(s) \\ b_2(s) \end{bmatrix} = \begin{bmatrix} s_{11}(s) & s_{12}(s) \\ s_{21}(s) & s_{22}(s) \end{bmatrix} \begin{bmatrix} a_1(s) \\ a_2(s) \end{bmatrix} \quad (12)
$$

where, for port voltages and currents $v_i(t)$ and $i_i(t)$, and port normalization (real) r_i; $i = 1,2$

$$
a_i = \frac{1}{2} \; (v_i/\sqrt{r_i} + i_i\sqrt{r_0})
$$

$$
b_i = \frac{1}{2} \; (v_i/\sqrt{r_i} - i_i\sqrt{r_0}) \quad (13)
$$

In (13), a_i and b_i are proportional to P_i and P_r, respectively, where P_i is the incident power and P_r the reflected power.

Then from (13) it is seen that a_i and b_i have units of $(\text{volt-amp})^{1/2}$. Of course functions of t and s are related through the (one-sided) Laplace transform. Thus from (12)

$$
b_2(s) = s_{21}(s)a_1(s) \Big|_{a_2(s) = 0} \quad (14)
$$

and

$$
\left| \frac{b_2(j\omega)}{a_1(j\omega)} \right|^2 = |s_{21}(j\omega)|^2 \quad (15)
$$

represents power transfer, specifically known as the transducer power gain. I.e. (15) gives the ratio of the average power delivered to the load resistance $r_2(a_2 = 0)$ to the maximum available power from a generator. In the time domain, (14) yields the impulse response when $a_1(s) = 1$, or

-12-

$$h(t) = b_2(t) = s_{21}(t) * \delta(t) = s_{21}(t) \qquad (16)$$

where $s_{21}(t)$ is the inverse Laplace transform of $s_{21}(s)$ and $*$ denotes convolution.

In the development which follows, the impulse response $h(t)$ is the inverse Laplace transform of the transmittance $s_{21}(s)$.

Since $s_{21}(s)$ is an analytic function for $s \geq 0$, it admits a Taylor series representation

$$s_{21}(s) = \sum_{i=0}^{\infty} \frac{a_i}{i!} s^i \qquad (17)$$

where the Taylor coefficients of (17) are the moments of $h(t)$, or since

$$s_{21}(s) = \int_0^{\infty} h(t)e^{-st}dt \qquad (18a)$$

$$\frac{d^n}{ds^n} s_{21}(s) = \int_0^{\infty} (-t)^n h(t)e^{-st}dt \qquad (18b)$$

$$a_n = \frac{d^n}{ds^n} s_{21}(0) = (-1)^n \int_0^{\infty} t^n h(t) \, dt \qquad (18c)$$

The mechanics of these computations are greatly simplified by approximating $h(t)$ in a piecewise linear fashion as shown in figure 2. With $h_k = h(t_k)$, the equation for the kth line segment is

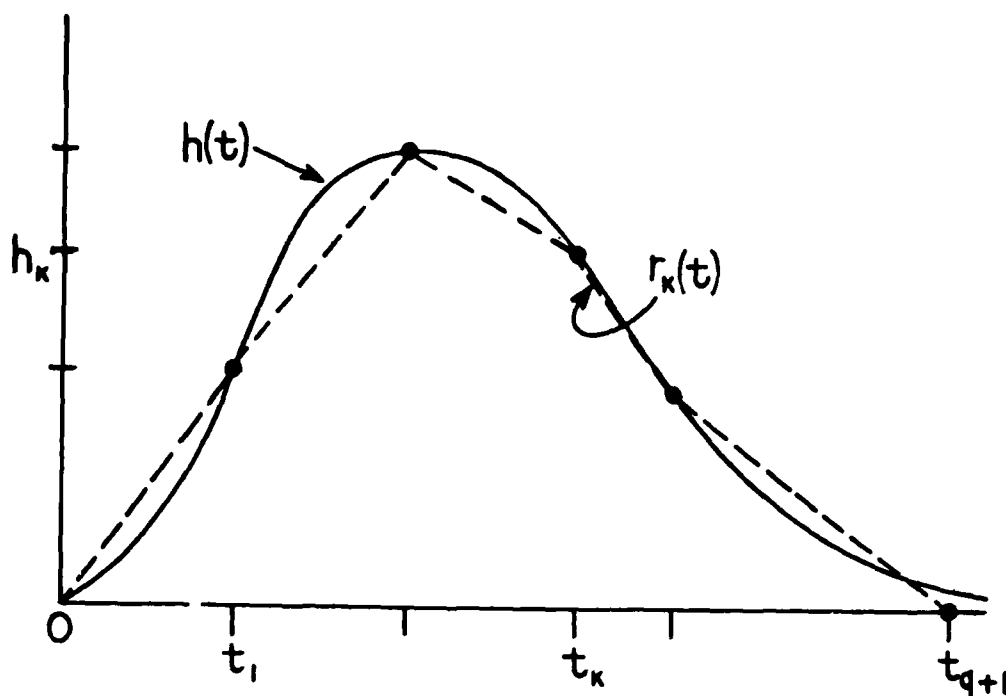$$r_k = m_k t + b_k \, , \quad t_k \leq t \leq t_{k+1}$$

Figure 2:   Piecewise-linear impulse response approximation

with $\quad m_k = \dfrac{h_{k+1} - h_k}{t_{k+1} - t_k}$ $\qquad\qquad$ (19)

and $\quad b_k = h_k - m_k t_k$

Under this approximation, the pth moment is easily computed by

$$s_{21}^{(p)}(0) \cong (-1)^p \sum_{i=0}^{q} \int_{t_i}^{t_{i+1}} t^p r_i(t)\, dt \qquad (20)$$

$$= \sum_{i=0}^{q} \left[\frac{m_i}{p+2} (t_{i+1}^{p+2} - t_i^{p+2}) + \frac{b_i}{p+1} (t_{i+1}^{p+1} - t_i^{p+1}) \right] \qquad (21)$$

Note from figure 2 that q is the penultimate sample of h(t).

In most practical application relatively few samples of h(t) are actually needed to represent its salient features such as rise time, fall time, and pulse width.

The crux of the problem is to find a realizable rational approximation to (17) such that under the specified frequency dependent terminations the desired h(t) is achieved as closely as possible. Using the notion of Pade' approximants, we seek polynomials P(s) and Q(s) of degrees m and n respectively, so that the rational function P(s)/Q(s) matches the first m + n terms of the infinite series [10]. Clearly and exact match of (17) cannot be generally obtained since P and Q must exactly include the constraints imposed by the generator and load as well as those of the lossless scattering matrix of the matching network (perhaps more appropriately, the pulse forming network).

Thus a solution is accepted if $s_{21}(s)$ as given by (5)

matches the series coefficients of (18c) as best as possible in a least squares sense. That is

minimize
over h(s)
$$s_{21}(h(s)) - \sum_{i=0}^{p} \frac{a_i}{i!} s^i \qquad (22)$$

In (22), p is the sum of the degrees of the generator and load denominator polynomials plus the desired order of the matching network (i.e., the degree of g(s)). Choosing p in this way takes best advantage of parasitic absorption.

The technique outlined here suggests a time domain approach to many of the classical broadband matching problems. For example, attention has been given recently to the design of linear phase or constant delay networks operating between frequency dependent terminations. The situation of a constant group delay translates into the simple time domain requirement that the impulse response be symmetric about some time t_0. Although causality will not allow perfect symmetry, the initial piecewise linear approximation for h(t) may be specified with perfect symmetry since (10) guarantees realizability. The final optimized result will thus approximate the constant delay property. Since the axis of symmetry t_0 is an input parameter, a design procedure for lossless delay lines becomes apparent.

IV. Group Delay Synthesis

Independent of the question of time domain synthesis, the approach outlined in section II suggests a direct approach for the design of networks with a specified group delay [6]. Referring again to equation (5), the group delay can be analytically computed as a rational function of ω [11]. Since

$$s_{21}(\omega) = |s_{21}(\omega)|e^{-j\psi(\omega)} \tag{23}$$

with $|s_{21}(\omega)| = |s_{21}(-\omega)|$ and $\psi(\omega) = -\psi(-\omega)$, then

$$\tau(\omega) = d\psi/d\omega = \frac{-1}{2j}\frac{d}{d\omega}\ln[s_{21}(j\omega)/s_{21}(-j\omega)] \tag{24}$$

Since the transmittance $s_{21}(s)$ as given by (5) is a rational function of s, the group delay $\tau(\omega)$ is computed as

$$\tau(\omega) = \text{Im}[P'(\omega)/P(\omega) - Q'(\omega)/Q(\omega)] \tag{25}$$

where $s_{21}(s) = P(s)/Q(s)$, $s = j\omega$;
the prime denoting differentiation with respect to ω, and $\text{Im}(\cdot)$ is the imaginary part. Since P and Q are polynomials, the differentiation is performed analytically and *no* numerical differentiation is required.

V. Optimization Procedure

For either the time domain or group delay synthesis procedures, the optimal matching network comes about from a numerical optimization procedure. Since the structure of the unknown equalizer E is formulated in such a way that realizability is guaranteed, any unconstrained optimization routine can be used to optimize the objective function. For the examples to follow a modified Levenberg-Marquandt algorithm is used to minimize

$$\epsilon = \sum_x [T(x_m) - T_i]^2 \qquad (26)$$

in a least squares sense [12,13]. $T(x_m)$ is the objective function evaluated for parameters x_m and T_i is the ideal value.

The computational procedure is as follows:

1. Referring to (10), fix upon the complexity of E by choosing n and k (recall n is the degree of h).

2. Take an (arbitrary) initial guess for h(s)
    $= h_0 + h_1 s + ... + h_n s^n$. Choosing $h_i = \pm 1$ works well in most instances.

3. Construct the even polynomial $g(s)g(-s) = h(s)h(-s) + s^{2k}$.

4. Perform spectral factorization of $g(s)g(-s)$ and isolate the left hand plane roots.

5. a) For time domain synthesis, optimize (22) using the Levenberg algorithm discussed.

b) For group delay equalization, minimize the quantity

$$\sum_{\substack{\text{over m} \\ \text{frequency} \\ \text{points}}} [\tau(\omega_m) - \tau_i]^2 \qquad (27)$$

in a least square sense, where τ_i is the desired delay at a frequency ω_i.

6. With the final optimized coefficients for h(s), construct S_e as in (10) and obtain a realization for E by usual synthesis procedures.

For numerical efficiency, all circuit element values are normalized to both frequency and impedance level. Thus in all circuit designs, if R', L' and C' are the actual element values, the normalized values are

$$R = R'/Z_0, \quad L = \omega_0 L'/Z_0, \quad C = \omega_0 C' Z_0,$$

corresponding to a normalized radian frequency ω/ω_0, $\omega = 2\pi f$. The quantity Z_0 is real (typically 50Ω). For the case of impulse response synthesis, the time domain amplitude and time axis are normalized as

$$T_0 h(t/T_0) \leftrightarrow H(s/\Omega_0) \qquad (28)$$
$$\Omega_0 = 1/T_0$$

As is usual with numerical procedures, a little forethought can often speed the optimization process. Examination of the moment expansion for the impulse response reveals that the zero[th] moment is the d.c. gain, certainly bounded by unity for a passive network. The first moment is the ratio of the d.c. delay to the d.c. gain.

VI. Examples

Example 1 (Time Domain Synthesis)

For many data transmission systems as well as in most radar applications, ringing in the pulse response should be minimal. This requires that the impulse response should not be negative, a property easily incorporated into the initial specification for h(t). In this way an acceptable compromise between rise time and overshoot can be reached.

The load impedance shown in figure 3 is a small signal model for a laser diode [14]. This load is to be matched to a 50Ω resistive generator as is to approximate the impulse response shown in figure 4, which is a five point approximation (circled points) to the first lobe of the ideal low pass filter impulse response

$$h_{ideal}(t) = \sin(t-\pi)/\pi(t-\pi), \quad 0 < t < 2\pi$$

Specifically, the initial approximation for h(t) is entered as

t	$h(t)$
0	0.0
1.57	0.202
3.14	0.318
4.71	0.202
6.28	0.0

Require the matching network to contain 3 elements (n=3), and clearly must be low pass in nature (k=0). With an abitrary initial guess for the coefficients of the polynomial h(s), the resulting optimized network has as its input reflection factor (50Ω normalization)

$$e_{11}(s) = \frac{2.08 - 3.11s + 1.69s^2 - .153s^3}{2.31 + 3.24s + 1.7s^2 + 0.153s^3}$$
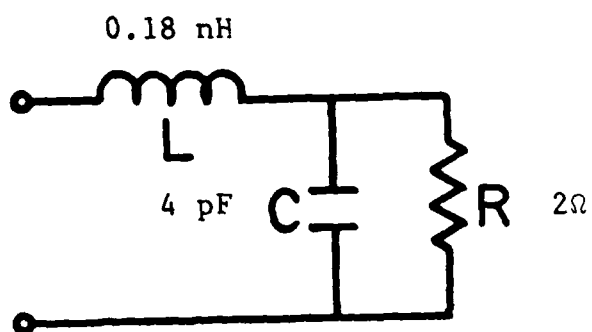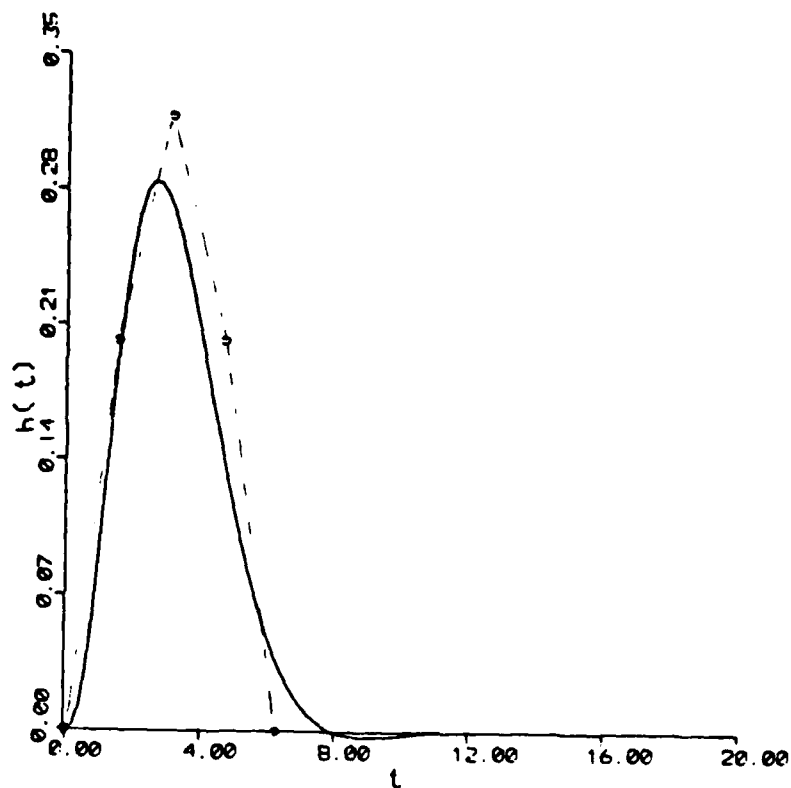
-20-

Figure 3: Laser diode model

Figure 4:   Impulse response, example 1

which is readily realized as a low pass ladder shown in figure 5. The resulting impulse response is shown in figure 4, where it is seen that even under the heavy load imposed by the diode the desired impulse response is closely achieved. For completeness, the gain and delay characteristics are shown in figure 6. Note that the group delay is relatively constant in the passband as a consequence of the approximate symmetry of the impulse response.
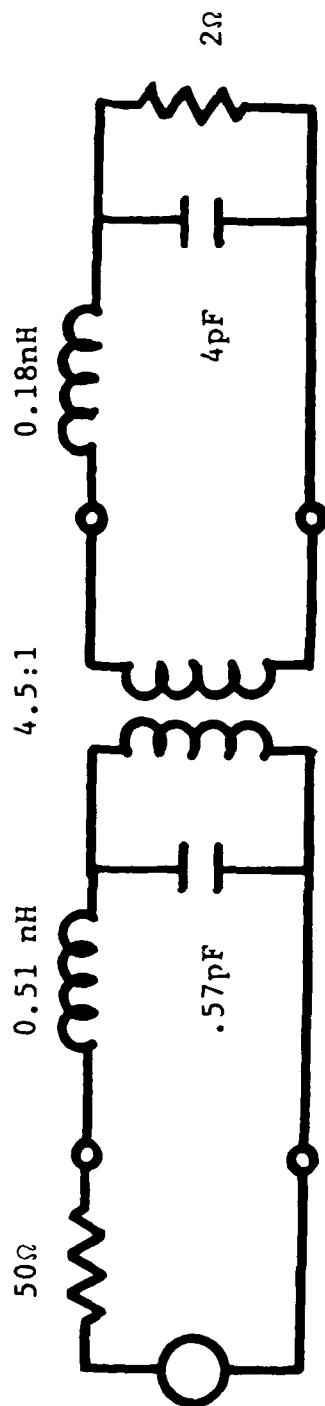
Figure 5: Realization, example 1
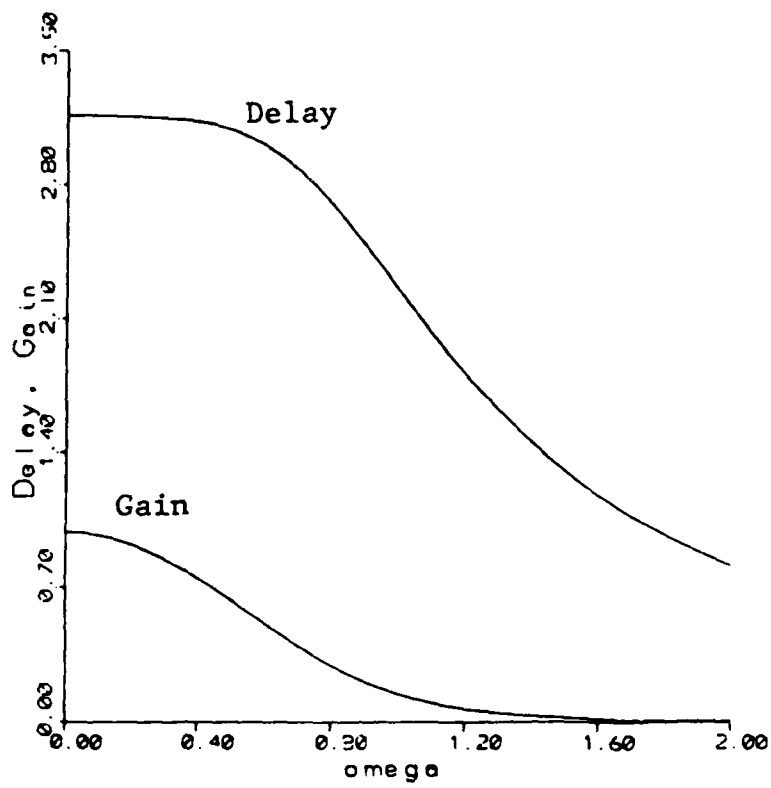
Figure 6:   Gain-delay, example 1

Example 2 (Group Delay Synthesis)

We consider here the recent example given by Zhu and Chen, where they design a matching network to yield a fourth-order maximally flat group delay characteristic. For the CAD procedure developed here, this is equivalent to sustaining the d.c. delay level in the passband. Specifically, we wish to design an all-pole low pass ($k=0$) equalizer which matches the generator impedance

$$z_g = 2/(s+2)$$

and the load impedance

$$z_1 = 0.2s + 7/(s+7)$$

so as to approximate a constant group delay of $\tau_0 = 2.34$ in the normalized frequency band $0 \leq \omega/\omega_0 \leq 1$. The matching network is to contain 3 elements ($n=3$) and have unity d.c. gain. An arbitrary initial guess for the coefficients of the polynomial $h(s)$ yields the optimized unit normalized input reflection coefficient,

$$e_{11}(s) = \frac{0.577s^3 + 0.104s^2 - .542s}{0.577s^3 + 1.69s^2 + 1.92s + 1}$$

This e_{11} is synthesized in the conventional way and is shown in figure 7. The gain and group delay characteristics are shown in figure 8 and the impulse response of the system in figure 9. Note that the group delay performance of the 3 element equalizer designed here is superior to that of Zhu and Chen's 4 element design, though the maximally flat character is no longer retained.
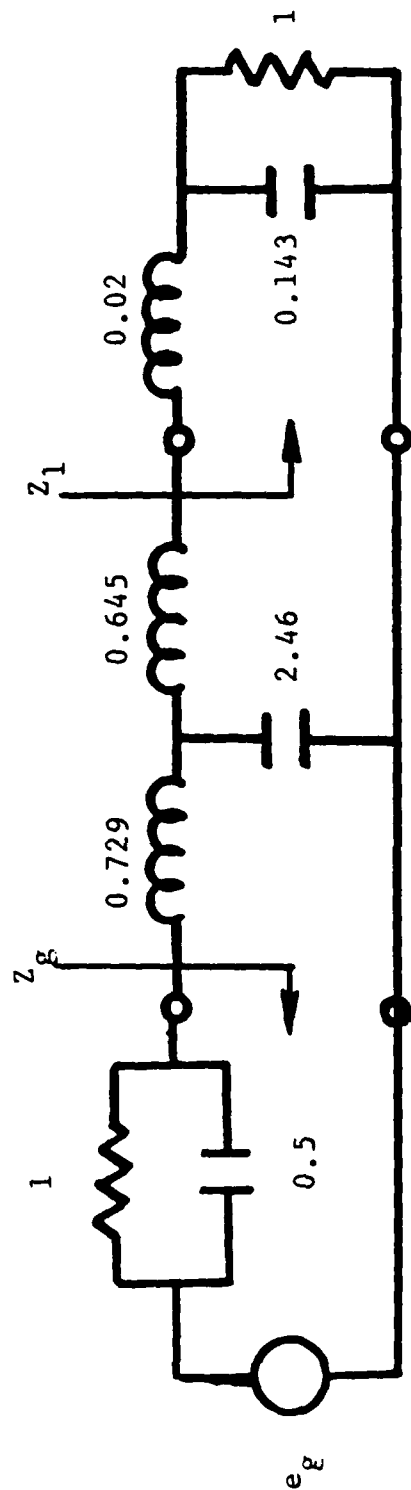
Figure 7: Realization, example 2
Elements specified in terms of normalized values:
R/R_o, $\omega_o CR_o$ and $\omega_o L/R_o$, R_o, ω_o arbitrary real positive
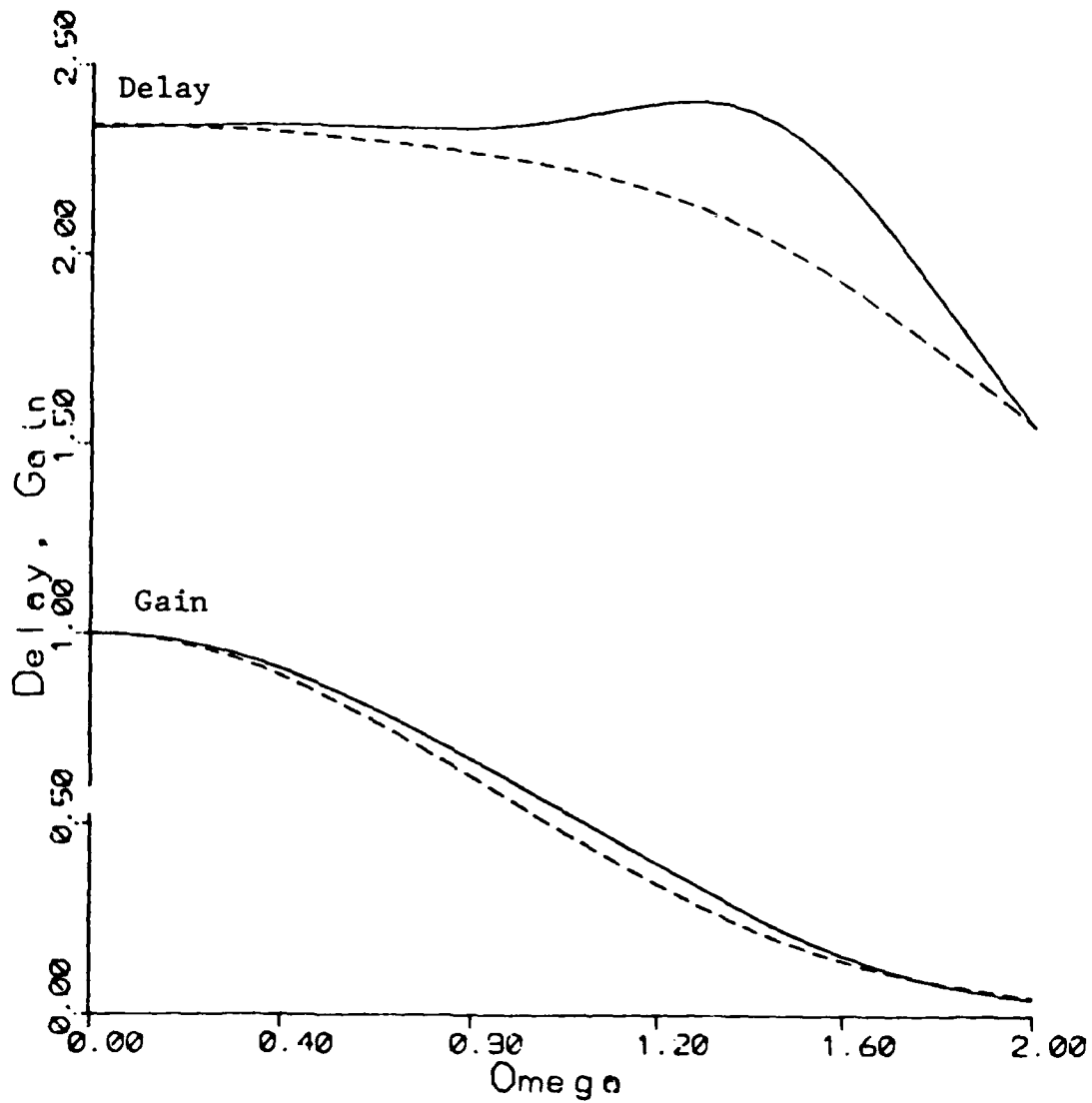constants.

Figure 8: Gain-Delay, example 2
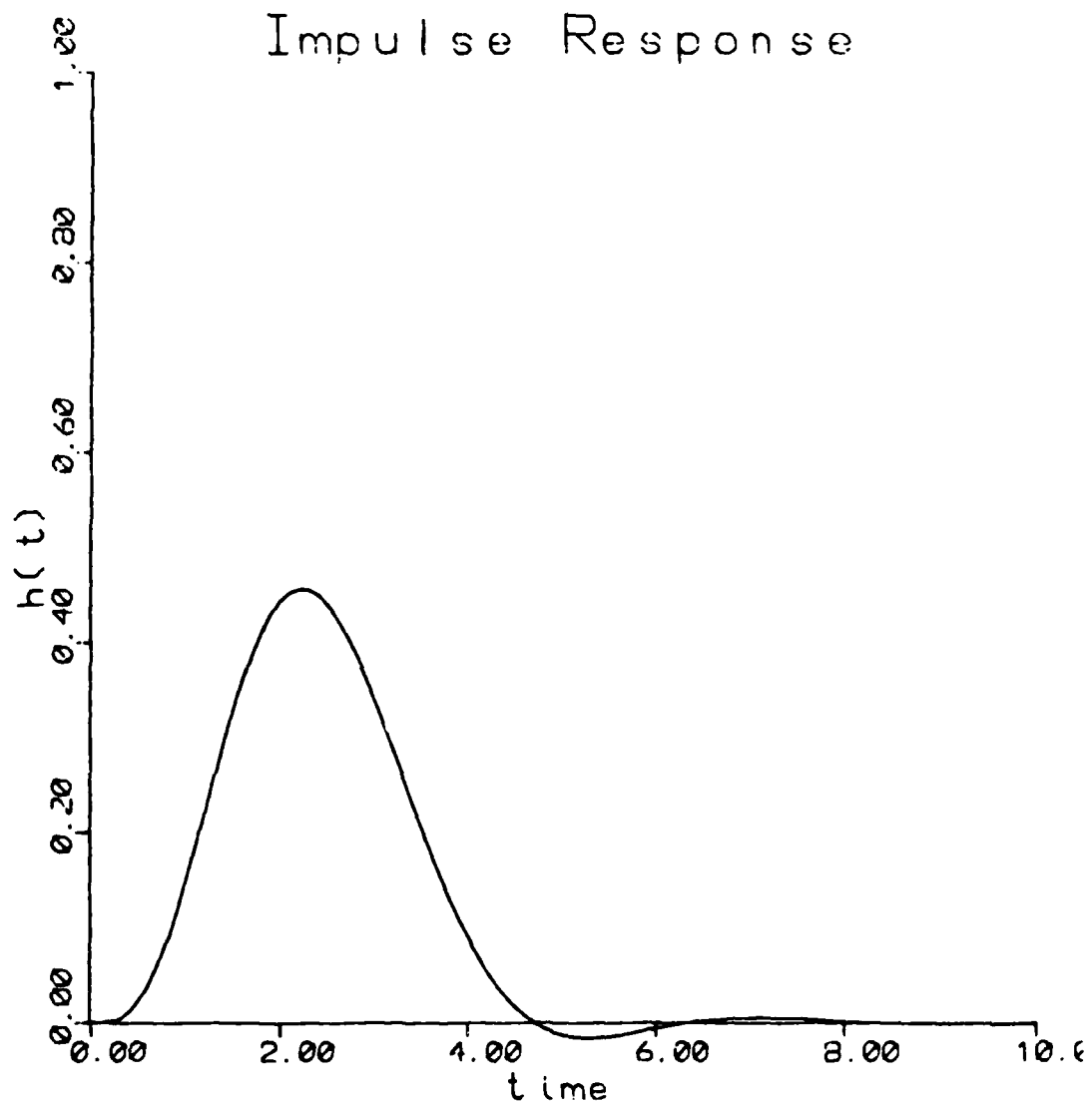(Dashed Curve for results of Zhu and Chen)

Figure 9:   Impulse response, example 2

Example 3: Impulse Response Synthesis; Active Case

Although the results thus far have been limited to the design of lossless matching networks operating between passive loads, these results are readily extended to the case of active networks. A relatively complete small signal model for a GaAs FET is shown in figure 10.[3] For the purposes of illustration, a somewhat simplified version of this model was used as shown in figure 11. A block diagram of the overall matching network is shown in figure 12, where E_F and E_B are the (lossless) front and back end matching networks each independently designed to achieve the desired performance goal, in this case a specific impulse response.

For the FET model of figure 11, the admittance matrix is readily obtained as

$$Y = \begin{bmatrix} s(C_{gs} + C_{gd}) & -sC_{gs} \\ -sC_{gs} + g_m & g_d + s(C_{ds} + C_{gd}) \end{bmatrix} \quad (29)$$

which then yields the real normalized scattering matrix

$$S = (1-Y)(1+Y)^{-1} \quad (30)$$

Then as in section II, if the generator, front-end equalizer, FET, back-end equalizer and load have transfer scattering matrices T_g, T_f, T_{FET}, T_b and T_e respectively then the overall transmittance is computed as a rational function and the design proceeds as described for the passive case. Since the front and back-end equalizers are designed independently, as a first step E_f is designed with E_b not present. Then with E_f fixed, E_b is determined.

---

[3]The model of figure 10 and its parameters were obtained from Mr. Phillip Wissell of ATT-Bell Labs through a private communication.

EQUIVALENT CIRCUIT OF GaAs FET CHIP
WITH 0.25μm GATE LENGTH

JS 8830-AS INCLUDING BOND WIRES
$V_{DS} = 3V$, $I_{DS} = 6mA$
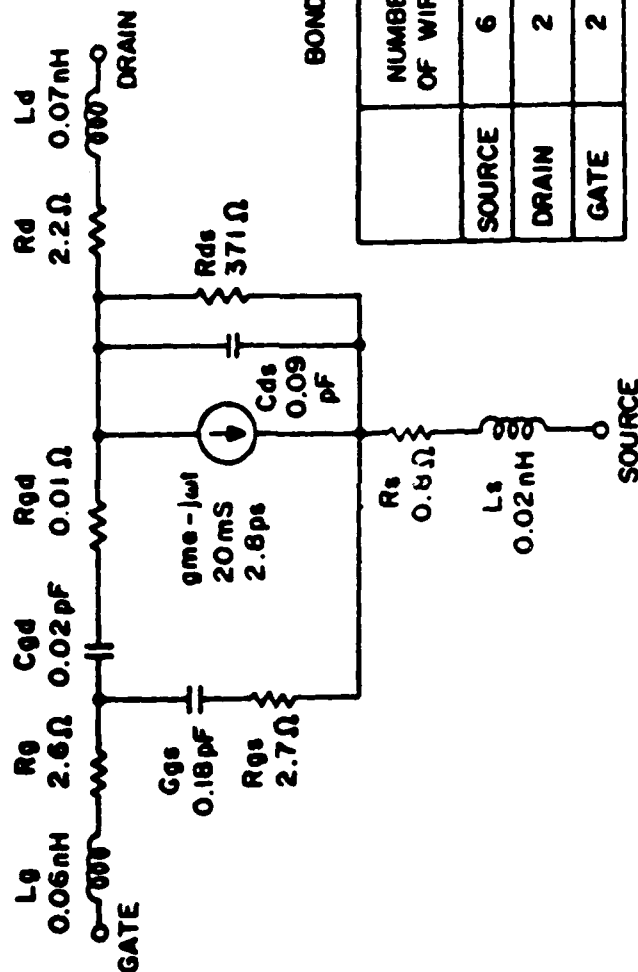
BOND WIRE DATA

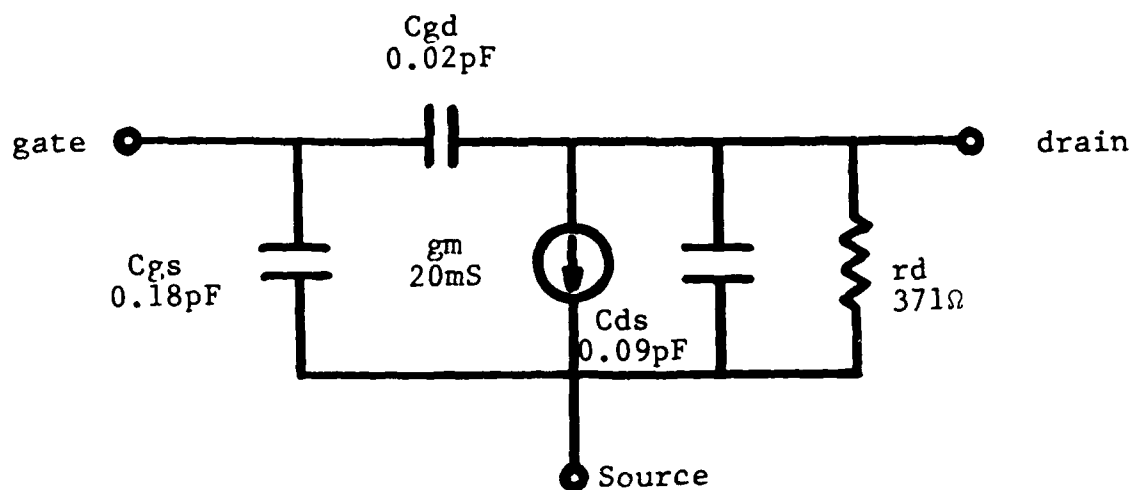|	NUMBER OF WIRES	LENGTH (APPROX.) (mm)	DIA. (μm)
SOURCE	6	0.3	25
DRAIN	2	0.4	25
GATE	2	0.4	25

Figure 10: General FET model

Figure 11: Simplified FET model
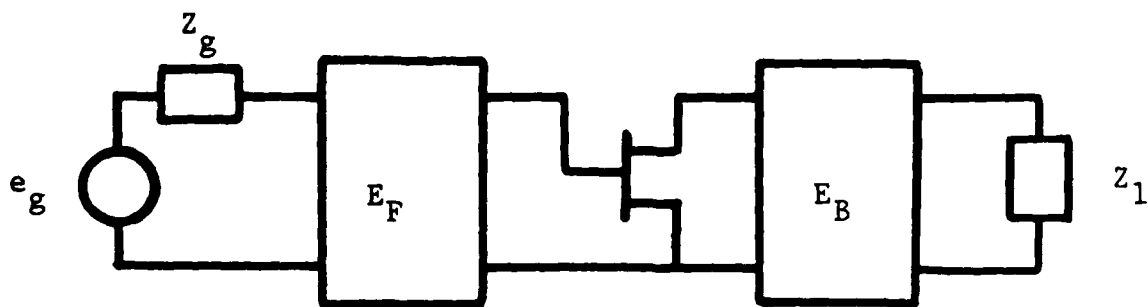
Figure 12:   Active matching

In the present example, the source impedance is assumed real (specifically 50Ω). Also, for practical considerations, the back-end equalizer is fixed to be a single series inductance representing a bond wire connecting the drain of the FET to the laser diode (as in figure 3).

The triangular waveform of figure 13 is to be approximated with a 3-element low pass front-end matching network and a 1-element back-end matching network as described above. The resulting optimized impulse response, gain-delay characteristic, and realization are shown in figures 13, 14 and 15 respectively.
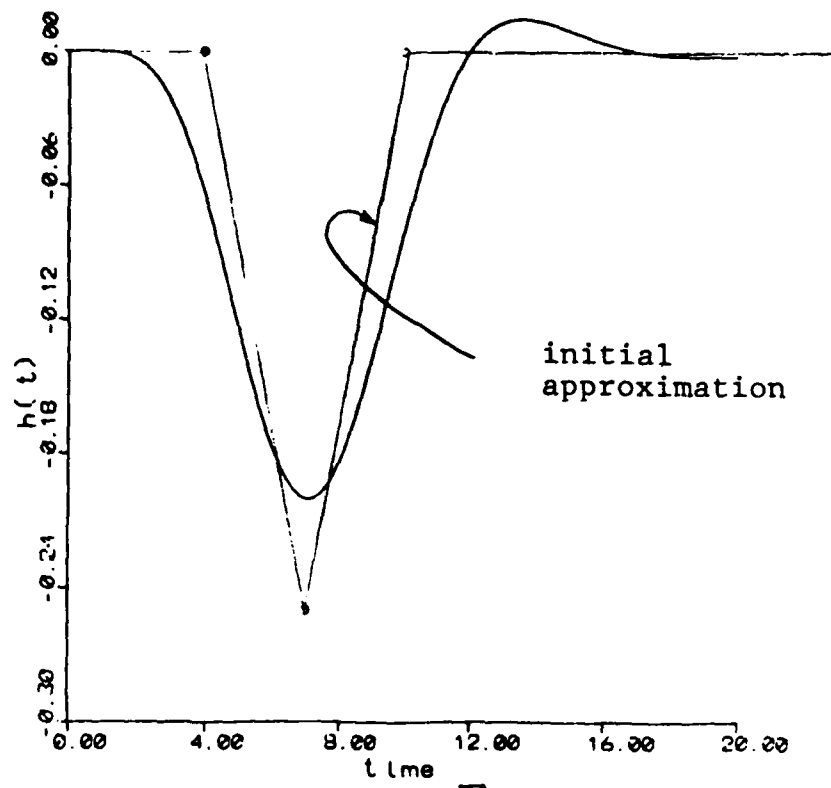
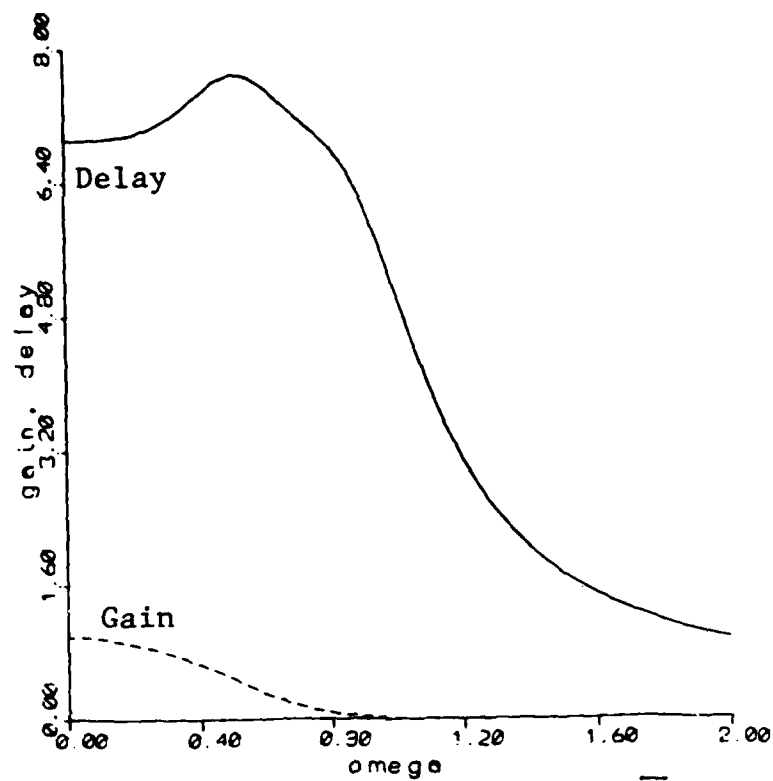Figure 13: Impulse response, example 3
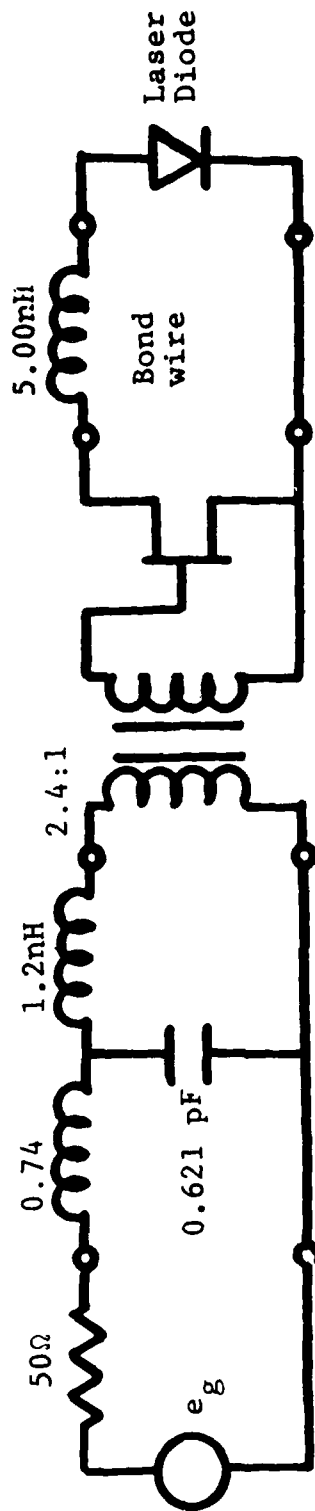
Figure 14: Gain-delay, example 3

Figure 15: Realization, example 3

Example 4: Group Delay Synthesis; Active Case

As in example 3, a resistive source network and laser diode load (figure 3) are to be matched using a 3-element low pass front-end and 1-element back-end equalizer with the FET of figure 11 so as to achieve constant group delay in the frequency band $0 \leq \omega/\omega_0 \leq 1$, $\omega_0 = 2\pi f_0$, $f_0 = 8$ GHz. The gain delay characteristics and impulse response for the overall optimized system are shown in figures 16 and 17, and corresponding realization in figure 18.
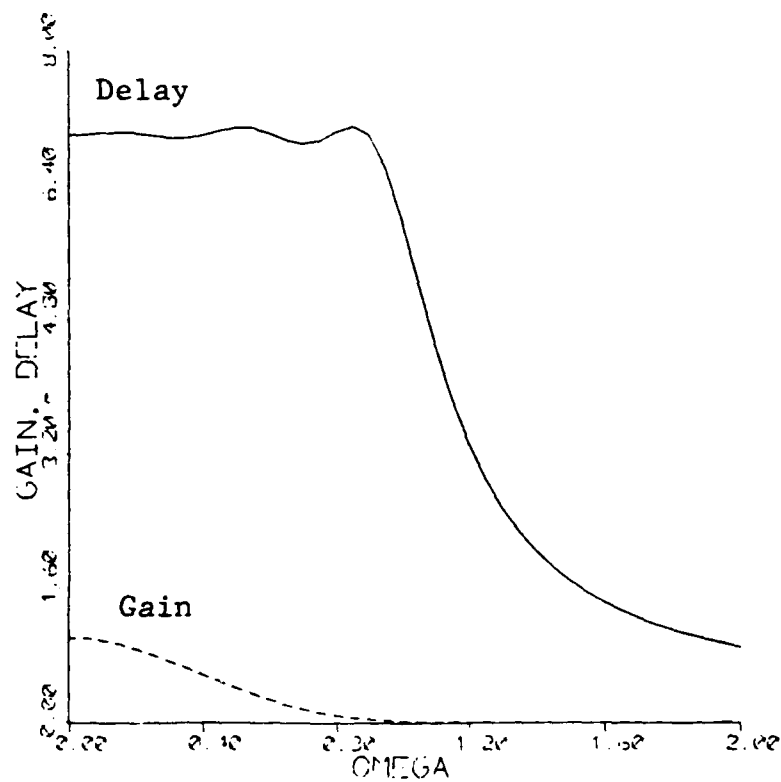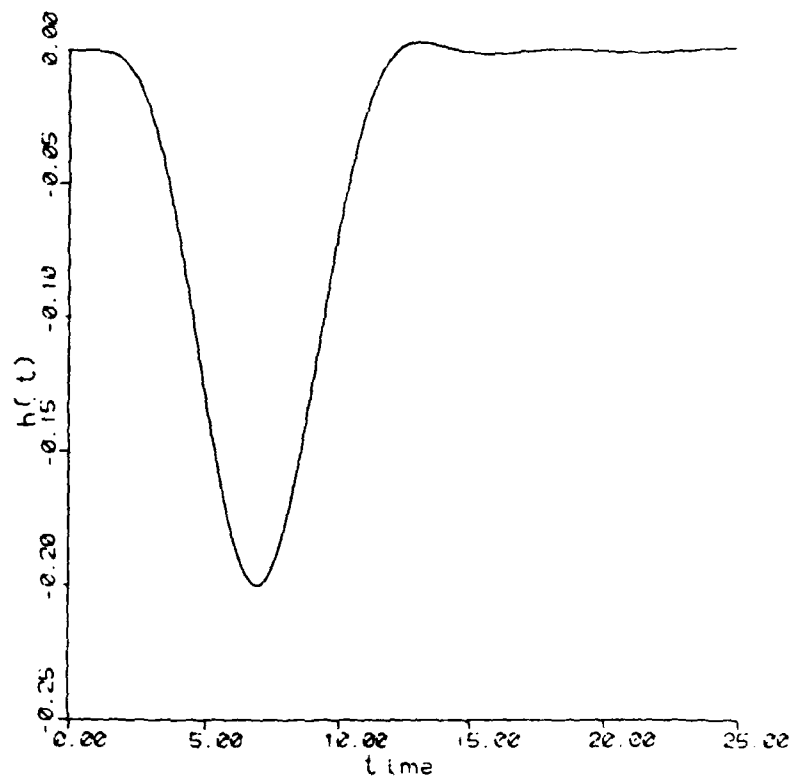
Figure 16: Gain-delay, example 4

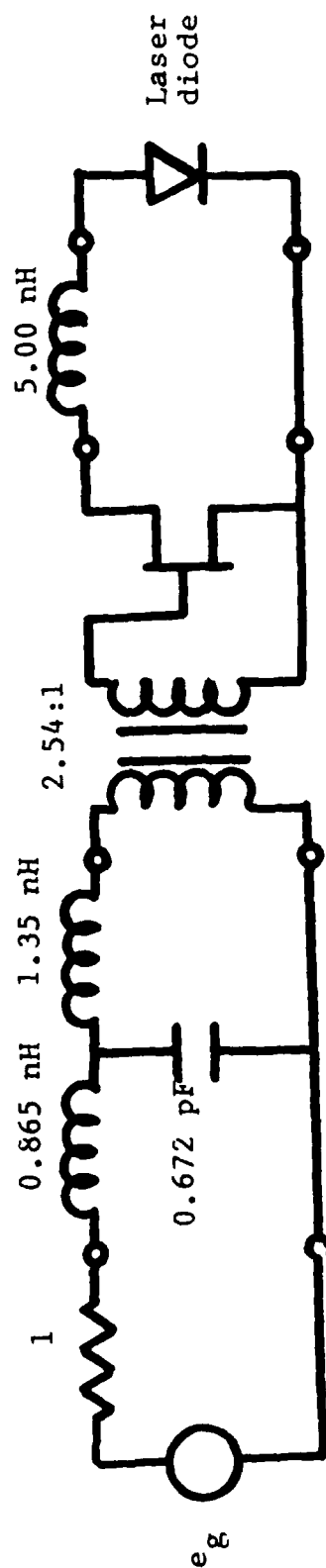Figure 17: Impulse response, example 4

Figure 18: Realization, example 4

VII Conclusions

It has been demonstrated that the basic computed aided design methods developed by Carlin and Yarman [2] can be extended to encompass a wide variety of general synthesis problems. Specifically, it has been seen that for arbitrary generator and load impedances the design of matching networks with a specified group delay is immediate. For the case of impulse response synthesis the procedure is a bit more subtle. This is essentially due to the restrictive nature of an impulse response in that it must consist of a sum of complex exponential functions, resulting in impulse response functions which are visibly similar to one another even though the corresponding frequency domain functions differ radically in appearance. From a practical standpoint however it has been seen that general pulse properties such as rise time, pulse width and ringing are immediately controllable.

The major difference between the techniques developed here and that of Carlin's is that lumped circuit models for the generator and load impedances as well as for the FET is required. This of course is to be expected since both frequency and time functions are differentiated in the design process and thus requiring analytic expressions as such. General guidelines concerning the constraints imposed by the load and generator on the impulse response are still unavailable.

-42-

VIII References

1. Carlin, H.J., and Amstutz, P.: 'On optimum broad-band matching', _IEEE Transactions on Circuits and Systems_, vol. 28, pp. 401-405, May 1981.

2. Carlin, H.J., and Yarman, B.S.: 'The double matching problem: analytic and real frequency solutions', _IEEE Transactions on Circuits and Systems_, vol. 30, pp. 15-28, January 1983.

3. H.J. Carlin "A New Approach to Gain-Bandwidth Problems," _IEEE Trans. Circuits and Systems_, Vol. CAS-24, pp. 170-175, April 1977.

4. B.S. Yarman and H.J. Carlin, "A Simplified 'Real Frequency' Technique Applied to Broad-Band Multistage Microwave Amplifiers", _IEEE Trans. on Microwave Theory and Techniques_, Vol. MTT-31, No. 3, March 1983, pp. 289-294.

5. D. J. Nicholson and H. Zmuda, "Matching Structures for High Speed Optical Communication", To be published in the _Proceedings of Society of Optical and Quantum Electronics Ninth International Conference on Lasers and Applications_, Orlando, Florida, Nov. 1986.

6. Zhu, Y.-S., and Chen, W.-K.: 'Broad-band matching with maximally flat group delay characteristic', _IEEE Transactions on Circuits and Systems_, vol. 34, pp. 658-668, June 1987.

7. L. Weinberg, _Network Analysis and Synthesis_, Huntington, New York; Robert E. Krieger Publishing Co., 1975.

8. E. Kuh and R. Rohver, _Theory of Linear Active Networks_, New York, Holden Day, 1967.

9. K. L. Su, <u>Time-Domain Synthesis of Linear Network</u>, Englewood Cliffs: Prentice Hall, Inc., 1971.

10. G. A. Baker, <u>Essentials of Pade' Approximants</u>, New York: Academic Press, 1975.

11. J. Neirynck, "The Attenuation Phase Compromise in the Polynomial Case," In <u>Network and Signal Theory</u>, London; Peter Perigrinus, 1973, pp. 215-200.

12. T.R. Cuthbert, Jr., <u>Optimization Using Personal Computers</u>, New York: John Wiley and Sons, 1987.

13. D. Humpherys, The <u>Analysis, Design, and Synthesis of Electrical Filters</u>, New York: Prentice Hall, 1970.

14. H. Zmuda, "Microwave Impedance Matching for Optical Devices", <u>Final Report</u>, United States Air Force – Universal Energy Systems Summer Faculty Research Program, Sept. 1986.